Organic & Biomolecular Chemistry

ROYAL SOCIETY OF CHEMISTRY

PAPER

View Article Online
View Journal | View Issue

Cite this: *Org. Biomol. Chem.*, 2024, **22**, 5930

Flavin-induced charge separation in transmembrane model peptides†

Samantha Wörner,[a] Pascal Rauthe,[b] Johannes Werner,[b] Sergii Afonin,[c] Anne S. Ulrich,[a,c] Andreas-Neil Unterreiner[b] and Hans-Achim Wagenknecht*[a]

Received 3rd June 2024,
Accepted 27th June 2024

DOI: 10.1039/d4ob00932k

rsc.li/obc

Hydrophobic peptide models derived from the α-helical transmembrane segment of the epidermal growth factor receptor were synthetically modified with a flavin amino acid as a photo-inducible charge donor and decorated with tryptophans along the helix as charge acceptors. The helical conformation of the peptides was conserved despite the modifications, notably also in lipid vesicles and multibilayers. Their ability to facilitate photo-induced transmembrane charge transport was examined by means of steady-state and time-resolved optical spectroscopy. The first tryptophan next to the flavin donor plays a major role in initiating the charge transport near the N-terminus, while the other tryptophans might promote charge transport along the transmembrane helix. These artificially modified, but still naturally derived helical peptides are important models for studying transmembrane electron transfer and the principles of photosynthesis.

Introduction

Photoinduced charge separation and charge transport processes in proteins belong to the most fundamental processes in biochemistry.[1] The most prominent examples are cyanobacterial, algal and plant photosystems, applying charge separation and charge transport to yield an electrochemical gradient across membranes.[2] Moreover, cryptochrome blue-light photoreceptors are responsible for biochemical photo-induced processes, including morphogenesis and entrainment of circadian rhythms,[3,4] and photolyases are related enzymes that repair UV-induced DNA damage.[4] The important feature of the latter types of enzymes is that they harbour a flavin as a photo-inducible chromophore and a redox-active cofactor.[5] Flavins can be photo-excited in the visible light range and have very distinct and powerful redox properties in three different charge transfer states. Hence, it is not surprising that riboflavin has also become an important photo-redox catalyst in organic synthetic chemistry.[6] Moreover, flavins are able to photo-induce charge transfer with the aromatic amino acids tryptophan and tyrosine as charge acceptors, which plays a major role in the generation of fully reduced flavins in DNA photolyases[7] and in the functional mechanism of cryptochromes.[8] In this context, studying protein-mediated transmembrane charge transport is an important research task.[9] Herein, we present new flavin-modified peptide models that are derived from the α-helical transmembrane fragment of the human epidermal growth factor receptor (EGFR, Fig. 1 and Table 1). The peptides were modified with a flavin amino acid as a photo-inducible charge donor (by generating an electron hole, acting as an electron acceptor), and decorated with a row of tryptophans along the helix as charge acceptors (*i.e.* electron donors). The ability of these patterns to facilitate photo-induced transmembrane charge transport was examined by means of stationary and time-resolved optical spectroscopy.

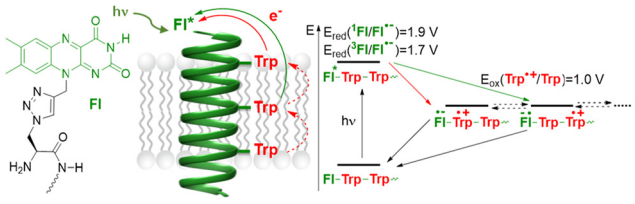

Fig. 1 Illustration of the functional peptide models for transmembrane charge transport derived from the EGFR and modified with flavin (Fl, green) as a photo-inducible charge donor and tryptophans (Trp, red) as charge acceptors.

[a]*Karlsruhe Institute of Technology (KIT), Institute of Organic Chemistry, Fritz-Haber-Weg 6, 76131 Karlsruhe, Germany. E-mail: Wagenknecht@kit.edu*
[b]*Institute of Physical Chemistry, Karlsruhe Institute of Technology (KIT), Fritz-Haber-Weg 2, 76131 Karlsruhe, Germany*
[c]*Karlsruhe Institute of Technology (KIT), Institute of Biological Interfaces (IBG2), POB 3640, 76021 Karlsruhe, Germany*

†Electronic supplementary information (ESI) available: Materials and methods, synthetic procedures, peptide synthesis and additional spectroscopic data. See DOI: https://doi.org/10.1039/d4ob00932k

Table 1 Sequences of the transmembrane model peptides **EGFRwt–EGFR$_{Fl}$5**, modified with the N-terminal flavin building block Fl (green) and with Trp (red). The transmembrane region of the peptide **EGFR$_{wt}$** is underlined

Peptide	Sequence	# of Trp
EGFR$_{wt}$	NH_2–GPKIPSIATGMVGALLLLLV VALGIGLFMRRRHIV–COOH	—
EGFR$_{Fl}$	NH_2–**Fl**–KIPSIATGMVGALLLLLV VALGIGLFMRRRHIV–COOH	—
EGFR$_{Fl}$1	NH_2–**Fl**–KIPS–**W**–ATGMVG–**W**–LLLLLV –**W**–ALGIGLYMRRRHIV–COOH	3
EGFR$_{Fl}$2	NH_2–**Fl**–K–**W**–PSIATG–**W**–VGALLL–**W**–LV VALGIGLYMRRRHIV–COOH	3
EGFR$_{Fl}$3	NH_2–**Fl**–K–**W**–PSIATG–**W**–VGALLL–**W**–LV VALG–**W**–GLYMRRRHIV–COOH	4
EGFR$_{Fl}$4	NH_2–**Fl**–K–**W**–PSI–**W**–TGM–**W**–GAL–**W**–LLL–**W**–VAL–**W**–IGLYMRRRHIV–COOH	6
EGFR$_{Fl}$5	NH_2–**Fl**–K–**W**–PS–**W**–ATG–**W**–VG–**W**–LLL–**W**–LV–**W**–ALG–**W**–GLYMRRRHIV–COOH	7

Results and discussion

As a representative model of an integral membrane protein, we selected the transmembrane segment of the human epidermal growth factor receptor (EGFR).[10] Our 33 amino acid sequence includes several residues from the extracellular juxtamembrane region (P^{641}–I^{643}), the hydrophobic α-helical TM-domain (P^{644}–M^{668}), and parts of the adjacent intracellular juxtamembrane region (R^{669}–V^{674}). The resulting transmembrane model peptides were modified at the N-terminus (amino acid position 641) to carry a redox-active isoalloxazine as the side chain. In contrast to the previously published flavin amino acid derived from L-lysine,[11] here we followed a more convergent approach for modifying peptides with chromophores using the Cu(I)-catalyzed "click"-type azide–alkyne cycloaddition. The Fmoc-protected flavin amino acid building block in the oxidized form of the chromophore was obtained – similar to our previous approach for attaching pyrenes,[12] aminophthalimide[13] and perylene bisimides[14] – by Cu(I)-catalyzed cycloaddition of the commercially available Fmoc-protected β-azido-L-alanine and propargyl-substituted flavin (see the ESI and Fig. S1–S7†).[15] The resulting amino acid building block was incorporated into the peptides **EGFR$_{Fl}$–EGFR$_{Fl}$5** (Table 1) using standard Fmoc-based solid-phase peptide synthesis protocols (Fig. S8–S15†). The peptides were purified (>90%) by reversed-phase HPLC and identified by MS (ESI-TOF). The wild-type **EGFR$_{wt}$** (G^{640}–V^{674}) lacks the N-terminal flavin and serves as a reference peptide to elucidate potential differences in the secondary structure caused by flavin modifications and other amino acid modifications in **EGFR$_{Fl}$–EGFR$_{Fl}$5** (Table 1).

Excitation of the flavin gives the single state ^{1}Fl* with a redox potential of E_{red} = 1.9 V *vs.* SHE (standard hydrogen electrode), and the subsequent intersystem crossing gives the triplet state ^{3}Fl* with a redox potential of E_{red} = 1.7 V *vs.* SHE.[5b] Both the states may serve as an excited electron acceptor for charge transfer[16] in combination with the naturally occurring amino acid tryptophan (Trp) as the electron donor. Trp has a lower redox potential (Trp: E_{ox} = 1.01 V *vs.* SHE) than the flavin excited states[17] and is able to quench the triplet state of the flavin unit. It is also well known to serve as a natural charge acceptor for the photo-induced charge transfer from flavins in DNA photolyases and as stepping stones for the incoherent charge hopping through these enzymes.[18] Such charge transfer pathways through cryptochromes were elucidated by Müller and Brettel *et al.* using time-resolved transient absorption spectroscopy.[19] This important function of Trp for peptide- and protein-mediated charge transfer was also extensively characterized by Giese *et al.* using poly-L-proline scaffolds as spectroscopic models.[20] Based on these results, we replaced several natural amino acids in **EGFR$_{Fl}$1–EGFR$_{Fl}$5** with an increasing number of Trp residues to mediate charge transport along the surface of these presumably α-helical model peptides. The first Trp residue was placed either at position 646 in **EGFR$_{Fl}$1**, which is approximately one helix turn away from the flavin-modified N-terminus, or at position 643 in **EGFR$_{Fl}$2–EGFR$_{Fl}$5**, which is closer to the N-terminus. Fluorescence quenching studies (*vide infra*) revealed that position 646 is too far away from the N-terminal flavin for efficient charge transfer. Thus, the first Trp was retained at position 643 in all further peptide sequences, and 1 Tyr and 2–3 additional Trp residues were placed at every 7th position in **EGFR$_{Fl}$2** and **EGFR$_{Fl}$3**. By this sequence design, Trp residues are oriented in proximity to each other at every second turn of the α-helix. Even more Trp residues were incorporated into **EGFR$_{Fl}$4** and **EGFR$_{Fl}$5**, such that every α-helix turn is occupied by a potential stepping stone for charge transport.

To ensure that the artificial flavin-modified N-terminal amino acid and more importantly the high number of Trp residues do not significantly alter the α-helical conformation or the membrane-embedded alignment of the EGFR-derived TM-domain, circular dichroism (CD) and oriented circular dichroism (OCD) spectra were recorded.[21] The CD spectra of **EGFR$_{Fl}$** and **EGFR$_{Fl}$1–EGFR$_{Fl}$5** in MeCN/H_2O (1 : 1) show the characteristic α-helical line-shape, with a maximum around 192 nm and two negative bands at 208 nm and 222 nm (Fig. 2 and S16†). These spectra are very similar to those of the wild-type peptide **EGFR$_{wt}$**, confirming that neither the N-terminal flavin building block nor the various Trp residues exert any significant perturbation on the global α-helical secondary conformation. This is a remarkable result in view of the high number of introduced modifications in particular by the Trp residues in **EGFR$_{Fl}$4** and **EGFR$_{Fl}$5** that were all placed along one face of the helix. Next, **EGFR$_{wt}$** and **EGFR$_{Fl}$1–EGFR$_{Fl}$5** were reconstituted in POPC bilayers with a peptide-to-lipid (P/L) ratio of 1 : 50 (mol : mol), by co-solubilization in a $CHCl_3$/MeOH (1 : 1) mixture and subsequent drying/rehydration. Large unilamellar vesicles were prepared from the peptide/lipid mixture in PBS buffer by extrusion. Although the CD spectra of these peptide-containing vesicles show a poor signal-to-noise ratio due to light scattering, they also confirm the α-helical secondary structure of the modified EGFR peptides in POPC vesicles. According to the CD spectra in solution, the peptides are found in their monomeric forms (the 208 nm band is lower than the 222 nm band). In the liposomes, however, they are clearly bundled

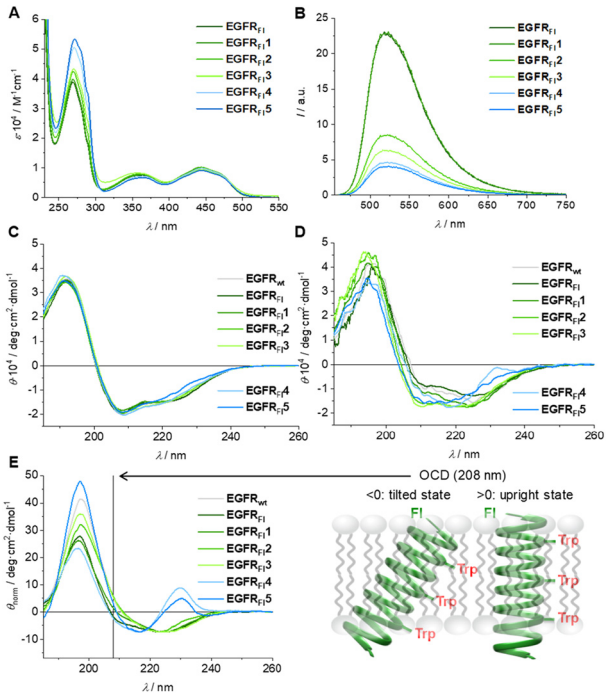

Fig. 2 (A) UV-Vis absorbance of $EGFR_{wt}$–$EGFR_{Fl}5$ (0.04 mM) in MeCN : H_2O (1 : 1) mixtures. (B) Fluorescence of $EGFR_{wt}$–$EGFR_{Fl}5$ (0.04 mM) in MeCN : H_2O (1 : 1) mixtures, λ_{exc} = 440 nm. (C) Circular dichroism (CD) of $EGFR_{wt}$–$EGFR_{Fl}5$ (0.1 mg mL^{-1}) in MeCN : H_2O (1 : 1). (D) Circular dichroism of $EGFR_{wt}$–$EGFR_{Fl}5$ in POPC bilayers at a P/L ratio of 1 : 50. (E) Oriented circular dichroism (OCD) of $EGFR_{wt}$–$EGFR_{Fl}5$ reconstituted in POPC bilayers at a P/L ratio of 1 : 50. The OCD spectra (25 °C) were normalized to their negative peak at 225 nm (except for $EGFR_{Fl}$ and $EGFR_{Fl}4$) to illustrate the similar line shapes (deviations at 233 nm are due to the increasing number of Trp residues, and deviations below 200 nm are commonly due to light scattering of the oriented samples). The positive band at the diagnostic λ = 208 nm supports the upright transmembrane orientation for **EGFRwt**, $EGFR_{Fl}1$–$EGFR_{Fl}3$ and $EGFR_{Fl}5$. Only $EGFR_{Fl}$ and $EGFR_{Fl}4$ show a slightly negative band at 208 nm indicating a more tilted transmembrane alignment, as illustrated on the right side.

(the 222 nm band is lower than the 208 nm band). The peptides were further examined in reconstituted membranes using a designated Oriented CD method (OCD), which can reveal the alignment of an α-helical peptide with respect to the lipid bilayer, *i.e.* whether the helix is inserted in the transmembrane, obliquely tilted, or surface-bound.[21] Macroscopically oriented membrane samples were prepared by (i) spreading the initial peptide–lipid solution onto a planar quartz glass sample holder, (ii) removing the organic solvent by drying overnight under vacuum, and (iii) full hydration of the sample in a humidity chamber. The oriented spectra were normalized to their negative peak at 225 nm to illustrate similar line shapes, except for $EGFR_{Fl}4$ and $EGFR_{Fl}5$. The signals of these two peptides start to deviate significantly from the other ones due to the increasing number of Trp residues, which contribute *per se* a positive band around 233 nm.[22] Nonetheless, the diagnostic positive signal at a wavelength of 208 nm serves as an indicator for the transmembrane alignment of peptides,[21] which fully supports the expected upright transmembrane orientation for $EGFR_{wt}$, $EGFR_{Fl}1$–$EGFR_{Fl}3$ and $EGFR_{Fl}5$. The model peptides $EGFR_{Fl}$ and $EGFR_{Fl}4$ show a diminished negative band at 208 nm, indicating a somewhat tilted membrane alignment of the peptides. By comparing the OCD signals with the CD signals, a decrease in the negative band can be confirmed, which indicates a properly inserted transmembrane orientation. For the peptides with the highest Trp content, a positive OCD band at ~230 nm emerges which can also be seen in the CD spectrum of the peptides $EGFR_{Fl}4$ and $EGFR_{Fl}5$. This band is in the absorption range of the Trps and their contribution to CD or OCD spectra is non-linear (*i.e.* non-proportional to the number of side chains). The observed OCD and CD bands are a specific spectral signature of the Trps in the local chiral environment of the peptides.

Steady-state fluorescence and fluorescence quantum yields were measured to obtain information on the charge transfer processes. The peptide $EGFR_{Fl}$ contains no Trp residues as charge acceptors, hence it will serve as a fluorescence reference. It shows a quantum yield of 0.13 in MeCN : H_2O (1 : 1) and 0.17 in POPC vesicles, which are our reference values without significant charge transfer contributions from any amino acid side chains. Surprisingly, the fluorescence quantum yield of $EGFR_{Fl}1$ in MeCN : H_2O (1 : 1) is nearly the same, although this peptide bears the nearest Trp residue just 5 amino acids (designed to be one helix turn) away from the flavin chromophore. This N-terminal region is located outside the membrane and non-helical (see Table 1 for the transmembrane regions of **EGFRwt**). It is not clear whether the N-terminus might have partially unravelled, but it is clear from our results that the first Trp as the charge acceptor must be placed closer to the flavin moiety, in order to efficiently induce charge transport along the transmembrane peptide. This condition was realized in $EGFR_{Fl}2$–$EGFR_{Fl}5$, with just a single lysine residue in between the N-terminal flavin and the first Trp. Accordingly, the fluorescence of $EGFR_{Fl}2$ is quenched to a quantum yield of 0.05 in MeCN : H_2O (1 : 1) and 0.08 in POPC vesicles. Additionally, the irradiation (5 min) of the peptides $EGFR_{wt}$ and $EGFR_{Fl}2$ using a 365 nm LED (Fig. S22†) revealed that the fast charge separation between Fl and Trp in the peptide $EGFR_{Fl}2$ protects its chromophore from photobleaching. The steady-state fluorescence quenching is further enhanced for $EGFR_{Fl}3$ in MeCN : H_2O to 0.04, respectively, which indicates an influence of the additional Trp residue on the charge transport along the helix. In POPC vesicles, $EGFR_{Fl}3$ shows a similar value within the higher experimental error. Overall, the data for EGFR-derived model peptides in POPC vesicles show the same trends as in the organic solvent, except for $EGFR_{Fl}1$. Here, the fluorescence is quenched compared to that for $EGFR_{Fl}$. This observation suggests that the peptide conformation in vesicles generates a better alignment of the flavin moiety relative to the Trp side chains, thus enabling a more efficient charge transport between flavin and the first Trp. Even more quenching is observed for $EGFR_{Fl}4$ and $EGFR_{Fl}5$, with a quantum yield of 0.03 in MeCN : H_2O (1 : 1) and 0.03–0.04 in POPC vesicles, due to the additional

number of Trp residues in these peptides. In particular, the second Trp at position 647 and 646 is closer to the first Trp at position 643. The latter observation indicates charge transport from the flavin at least to the second Trp residue in these peptides. The steady-state fluorescence measurements, in MeCN : H_2O (1 : 1), show that the number of Trp residues in **$EGFR_{Fl}$3–$EGFR_{Fl}$5** correlates with the extent of fluorescence quenching. In POPC vesicles, the same trend is observable, although the experimental errors for the fluorescence quantum yields are higher. This observation indicates that even the Trp residues beyond the first and second Trp are involved in the charge transport, thereby providing a continuous channel along the helix surface for charge transport across the lipid bilayer of the POPC vesicles.

The absorption spectrum of the peptides is typical for flavin systems, with two characteristic band peaks at 360 and 445 nm.[23] Introducing additional Trp units into the peptide sequence does not significantly change the position or the shape of this moiety. Time-resolved absorption measurements were carried out for **$EGFR_{Fl}$** and the Trp modified systems **$EGFR_{Fl}$2–$EGFR_{Fl}$5**. The corresponding contour plots and transient absorption (TA) spectra are provided in the ESI (Fig. S16 to S20†). Our analysis begins with **$EGFR_{Fl}$** (Fig. 3 left), as the reference system, lacking Trp side chains, *i.e.* without charge acceptors. The TA data exhibit characteristic temporal evolution of flavins, featuring two excited state absorption (ESA) bands at 500 nm and 700 nm, along with negative pump-induced response including ground state bleach (GSB) at around 430 nm and a stimulated emission (SE) at 550 nm. These observations align well with the TA spectra of flavin derivatives reported[26] and our previous investigations of flavin-modified amino acids with a different peptide secondary structure as a reference (polyproline helix instead of α-helix).[23] Global analysis identifies the primary feature as the lifetime of the first singlet excited state, exceeding 1.2 ns – the maximum delay achievable with our setup. This time constant is also evident for the Trp-modified peptides **$EGFR_{Fl}$2–$EGFR_{Fl}$5** (for **$EGFR_{Fl}$2** see Fig. 3 right, for **$EGFR_{Fl}$3–$EGFR_{Fl}$5** see Fig. S22†). However, an additional broad ESA emerges starting at 500 nm and extending to longer wavelengths with a time constant of approximately 2 ps (see τ_1 in Table 2). Notably, this band is clearly dependent on the presence of Trp. Based on the reference absorption spectra for all possible flavin and Trp radical intermediates reported by Brettel *et al.*[8a] we assign the ESA band at 500–650 nm to the Trp radical cation that gives spectroscopic evidence for the charge transfer in the peptides **$EGFR_{FL}$2–$EGFR_{FL}$5**. It is important to note here that we observed the Trp radical cation, and not the deprotonated Trp radical, because the latter has different spectral characteristics and its absorption is more blue-shifted with a broad maximum at 510 nm. It is often observed that protonated intermediates exhibit red-shifted spectra compared to their deprotonated counterparts, as exemplified by the Trp radical.[19] In contrast, the decay of the spectral feature, reflected by τ_1, is found to be much faster (tens of ps compared to hundreds of ps or longer). This discrepancy provides an opportunity for further investigations of such model systems. Previous studies by Bialas *et al.*[24] examining a similar flavin/tryptophan system in α-helical peptide bundles reported triplet state formation with an ESA band at 520–600 nm after 800 ps to 1 ns, making triplet state formation within 2 ps in our peptides improbable. Moreover, the spectral signature of radical formation differs, exhibiting a slightly blue-shifted maximum and a μs timescale.[29] Based on these spectroscopic differences and the ps dynamics, we assume that the CT in our modified peptides **$EGFR_{Fl}$2–$EGFR_{Fl}$5** is induced by the singlet excited state of the flavin. This charge transfer on the ps timescale was not observed by Bialas *et al.* in their peptide helix bundles,[24] because the distance between the flavin (in position 9) and the Trp (in position 13) was too big (3 intervening amino acids) for CT, similar to our peptide **$EGFR_{FL}$1** (4 intervening amino acids) in which we could not get any spectroscopic evidence for CT, too. It has been recognized that biexponential fitting may inadequately capture all relevant processes such as vibrational cooling,[26] internal conversion/conical intersection,[25] intersystem crossing,[24,26] radical formation[29] and redox states, among others.[27] Consequently, a more detailed investigation, potentially complemented by other techniques such as femtosecond fluorescence upconversion and multiple state analysis, is warranted.[28]

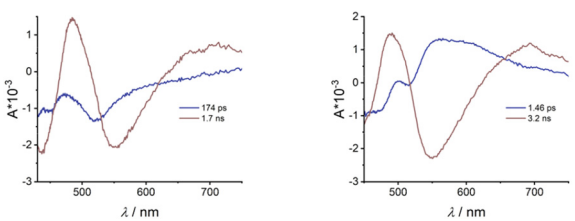

Fig. 3 Decay-associated difference spectra (DADS) after biexponential fitting of **$EGFR_{Fl}$** (left) and **$EGFR_{Fl}$2** (right) following 400 nm fs excitation.

Table 2 Fluorescence quantum yields Φ_F in MeCN : H_2O = 1 : 1 and in POPC vesicles from steady-state experiments in comparison with the τ_1 in MeCN : H_2O = 1 : 1 from global fits of time-resolved measurements

Peptide	Φ_F in MeCN : H_2O = 1 : 1	τ_1 in ps in MeCN : H_2O = 1 : 1	Φ_F [b] in POPC vesicles
$EGFR_{Fl}$	0.13	—[a]	0.17
$EGFR_{Fl}$1	0.13	—[a]	0.10
$EGFR_{Fl}$2	0.05	1.46	0.08
$EGFR_{Fl}$3	0.04	1.52	0.08
$EGFR_{Fl}$4	0.03	1.99	0.03
$EGFR_{Fl}$5	0.03	1.87	0.04

[a] No CT. [b] Due to scattered light, the accuracy is lower than for Φ_F in MeCN : H_2O = 1 : 1.

Experimental

All experimental methods and additional data are provided in the ESI.†

Conclusions

In conclusion, we have designed a series of new peptides, based on the EGFR transmembrane helix, which enable electron-transport along a dedicated path of Trp side chains across the lipid bilayer. This functional design was achieved by labeling the peptides with a flavine-modified amino acid at the N-terminus, which can initiate photo-induced charge separation. Several tryptophan units are decorated along the helix as charge acceptors, to serve as potential stepping stones for the charge transport. Notably, the helical conformation of the EGFR-derived peptides was conserved, despite the flavin and tryptophan modifications. The transmembrane charge separation was evidenced by both steady-state fluorescence and time-resolved laser spectroscopy. The close distance between the flavin and the first Trp in **EGFR$_{Fl}$2** (compared to **EGFR$_{Fl}$1**) is an important structural prerequisite for efficient charge separation in these α-helical peptides. Both in MeCN : H_2O (1 : 1) and in POPC vesicles, the number of Trp residues in **EGFR$_{Fl}$2** to **EGFR$_{Fl}$5** correlates with the fluorescence quenching from steady-state experiments and the charge transfer lifetimes determined by the time-resolved measurements. These experiments indicate that also the second Trp residue and those beyond are involved in charge transport and thus provide a designated pathway for charge transport. The similarity of the spectroscopic results from MeCN : H_2O and unilamellar POPC vesicles shows that these structurally designed transmembrane peptides have the potential to transport charge across the lipid membrane. Using advanced time-resolved spectroscopy, the charge-separated state was identified from the singlet state of the excited flavin and from the fingerprint of the Trp radical cation. Remarkably, the transient data of this Trp radical cation in the charge-separated states, as derived, correlate reasonably well with the fluorescence quantum yields. Taken together, these well-designed, yet naturally derived α-helical peptides are valuable models for not only studying specific transmembrane charge transfer, but also to develop artificial photosynthesis in general.

Author contributions

Samantha Wörner synthesized the peptides and analysed them by steady-state spectroscopy. Pascal Rauthe and Johannes Werner performed the time-resolved spectroscopy. Sergii Afonin helped with the peptide reconstitution and oriented CD measurements. Anne S. Ulrich, Andreas-Neil Unterreiner and Hans-Achim Wagenknecht supervised the research and wrote the manuscript.

Data availability

The data supporting this article have been included as part of the ESI.†

Conflicts of interest

There are no conflicts to declare.

Acknowledgements

Financial support by the Deutsche Forschungsgemeinschaft (Graduiertenkolleg 2039/2) and KIT is gratefully acknowledged. We also appreciate the advice and support of Dr Parvesh Wadhwani, Andrea Eisele and Kerstin Scheubeck in the PepSyLab of IBG2, and of Dr Jochen Bürck and Bianca Posselt in the CD lab of IBG2.

References

1 H. B. Gray and J. R. Winkler, *Q. Rev. Biophys.*, 2003, **36**, 341–372.
2 B. A. Barry, *J. Photochem. Photobiol., B*, 2011, **104**, 60–71.
3 (*a*) C. Lin and D. Shalitin, *Annu. Rev. Plant Biol.*, 2003, **54**, 469–496; (*b*) R. Stanewsky, *J. Neurobiol.*, 2003, **54**, 111–147.
4 A. Sancar, *Chem. Rev.*, 2003, **103**, 2203–2237.
5 (*a*) S. L. J. Tan and R. D. Webster, *J. Am. Chem. Soc.*, 2012, **134**, 5954–5964; (*b*) P. F. Heelis, *Chem. Soc. Rev.*, 1982, **11**, 15–39; (*c*) S. Ghisla, W. C. Kenney, W. R. Knappe, W. McIntire and T. P. Singer, *Biochemistry*, 1980, **19**, 2537–2544.
6 (*a*) T. Hering, B. Mühldorf, R. Wolf and B. König, *Angew. Chem., Int. Ed.*, 2016, **55**, 5342–5345; (*b*) H. Gruß, C. Belu, L. M. Bernhard, A. Merschel and N. Sewald, *Chem. – Eur. J.*, 2019, **25**, 5880–5883; (*c*) A. Rehpenn, A. Walter and G. Storch, *Synthesis*, 2021, **53**, 2583–2593.
7 (*a*) T. Carell, L. T. Burgdorf, L. M. Kundu and M. Cichon, *Curr. Opin. Chem. Biol.*, 2001, **5**, 491–498; (*b*) M. Müller and T. Carell, *Curr. Opin. Struct. Biol.*, 2009, **19**, 277–285.
8 (*a*) P. Müller, E. Ignatz, S. Kiontke, K. Brettel and L.-O. Essen, *Chem. Sci.*, 2018, **9**, 1200–1212; (*b*) P. Müller, J. Yamamoto, R. Martin, S. Iwai and K. Brettel, *Chem. Commun.*, 2015, **51**, 15502–15505; (*c*) F. Lacombat, A. Espagne, N. Dozova, P. Plaza, P. Müller, K. Brettel, S. Franz-Badur and L.-O. Essen, *J. Am. Chem. Soc.*, 2019, **141**, 13394–13409.
9 (*a*) D. J. R. Lane and A. Lawen, *BioFactors*, 2009, **34**, 191–200; (*b*) J. Hinks, Y. Wang, W. H. Poh, B. C. Donose, A. W. Thomas, S. Wuertz, S. C. J. Loo, G. C. Bazan, S. Kjelleberg, Y. Mu and T. Seviour, *Langmuir*, 2014, **30**, 2429–2440; (*c*) G. Goparaju, B. A. Fry, S. E. Chobot, G. Wiedman, C. C. Moser, P. L. Dutton and B. M. Discher, *Biochim. Biophys. Acta*, 2016, **1857**, 503–512.
10 E. V. Bocharov, P. E. Bragin, K. V. Pavlov, O. V. Bocharova, K. S. Mineev, A. A. Polyansky, P. E. Volynsky, R. G. Efremov and A. S. Arseniev, *Biochemistry*, 2017, **56**, 1697–1705.
11 T. Carell, H. Schmid and M. Reinhard, *J. Org. Chem.*, 1998, **63**, 8741–8747.

12 (*a*) S. Hermann, D. Sack and H.-A. Wagenknecht, *Eur. J. Org. Chem.*, 2018, 2204–2207; (*b*) S. Hermann and H.-A. Wagenknecht, *J. Pept. Sci.*, 2017, **23**, 563–566.
13 S. Wörner, F. Rönicke, A. S. Ulrich and H.-A. Wagenknecht, *ChemBioChem*, 2020, **21**, 618–622.
14 D. Sack and H.-A. Wagenknecht, *Eur. J. Org. Chem.*, 2021, 6400–6407.
15 (*a*) R. Kumar, R. K. Arigela, S. Samala and B. Kundu, *Chem. – Eur. J.*, 2015, **21**, 18828–18833; (*b*) D. Shetty, J. M. Jeong, C. H. Ju, Y. J. Kim, J.-Y. Lee, Y.-S. Lee, D. S. Lee, J.-K. Chung and M. C. Lee, *Bioorg. Med. Chem.*, 2010, **18**, 7338–7347.
16 U. Megerle, M. Wenninger, R.-J. Kutta, R. Lechner, B. König and E. Riedle, *Phys. Chem. Chem. Phys.*, 2011, **13**, 8869–8880.
17 E. J. Land and A. J. Swallow, *Biochemistry*, 1969, **8**, 2117–2125.
18 T. Carell, L. T. Burgdorf, L. M. Kundu and M. Cichon, *Curr. Opin. Chem. Biol.*, 2001, **5**, 491–498.
19 P. Müller, E. Ignatz, S. Kiontke, K. Brettel and L.-O. Essen, *Chem. Sci.*, 2018, **9**, 1200–1212.
20 (*a*) N. P.-A. Monney, T. Bally and B. Giese, *J. Phys. Org. Chem.*, 2015, **28**, 347–353; (*b*) A. Heck, P. B. Woiczikowski, T. Kubar, K. Welke, T. Niehaus, B. Giese, S. Skourtis, M. Elstner and T. R. Steinbrecher, *J. Phys. Chem. B*, 2014, **118**, 4261–4272; (*c*) M. Cordes and B. Giese, *Chem. Soc. Rev.*, 2009, **38**, 892–901.
21 J. Bürck, P. Wadhwani, S. Fanghänel and A. S. Ulrich, *Acc. Chem. Res.*, 2016, **49**, 184–192.
22 (*a*) D. Andersson, U. Carlsson and P.-O. Freskgård, *Eur. J. Biochem.*, 2001, **268**, 1118–1128; (*b*) R. W. Woody, *Biopolymers*, 1978, **17**, 1451–1467.
23 S. Wörner, J. Leier, N. C. Michenfelder, A.-N. Unterreiner and H.-A. Wagenknecht, *ChemistryOpen*, 2020, **9**, 1264–1269.
24 C. Bialas, D. T. Barnard, D. B. Auman, R. A. McBride, L. E. Jarocha, P. J. Hore, P. L. Dutton, R. J. Stanley and C. C. Moser, *Phys. Chem. Chem. Phys.*, 2019, **21**, 13453–13461.
25 Y. Ai, C. Zhao, J. Xing, Y. Liu, Z. Wang, J. Jin, S. Xia, G. Cui and X. Wang, *J. Phys. Chem. A*, 2018, **122**, 7954–7961.
26 R. J. Stanley, *Antioxid. Redox Signal.*, 2001, **3**, 847–866.
27 B. Zhuang, U. Liebl and M. H. Vos, *J. Phys. Chem. B*, 2022, **126**, 3199–3207.
28 B. Zhuang, D. Seo, A. Aleksandrov and M. H. Vos, *J. Am. Chem. Soc.*, 2021, **143**, 2757–2768.
29 H.-A. Wagenknecht, E. D. A. Stemp and J. K. Barton, *Biochemistry*, 2000, **39**, 5483–5491.